THE PERKIN-ELMER CORPORATION
AEROSPACE DIVISION
2855 Metropolitan Place Pomona, California 91767

FINAL REPORT

ATMOSPHERIC CONTAMINANT SENSOR

BOOK 1 OF 3

By Burton W. Scott
and J. H. Stuart

April 1972

Perkin-Elmer SPO No. 30249

OFFICE OF PRIME RESPONSIBILITY

EB7

Prepared for
NATIONAL AERONAUTICS AND SPACE ADMINISTRATION
Manned Spacecraft Center
R&D Procurement Branch
Houston, Texas

PRECEDING PAGE BLANK NOT FILMED

TABLE OF CONTENTS

LIST OF ILLUSTRATIONS

LIST OF ILLUSTRATIONS (Cont)

INTRODUCTION

Under the terms of contract NAS9-12066 the Perkin-Elmer Corporation, Aerospace Division, designed and fabricated a mass spectrometer system for use as an atmospheric monitor for submarine use. The period of performance and cost were minimized by utilizing, as much as possible, the design of the Mass Spectrometer Sensor System (MSSS), which was designed under contract NAS9-9799 for NASA/MSC. Certain modifications were necessary, however, because of some unique aspects of the submarine atmosphere monitoring problem. The performance design goals are presented in Table 1. The operation of the system is essentially automatic, providing continuous display of the partial pressures of the principal atmospheric constituents and a pushbutton update display of two freon trace contaminants. The freon update cycle takes 15 or 30 seconds, depending on which are measured. Trouble free, long term, reliable operation, and ease of maintenance were the primary system requirements. An additional design goal was a mechanical configuration that can withstand the MIL-S-901 shock test.

The requirement of the freon detection with high sensitivity and high resolution made redesign of the overall analyzer housing and magnet necessary. The ion source from the MSSS was essentially unmodified, representing a great savings in design effort.

A basic description of the system is included in the Operations and Maintenance Manual and will not be repeated here.

TABLE 1. SYSTEM PERFORMANCE AND DESIGN GOALS

System performance shall, as a design goal, be maintained within the limits specified during operation in the anticipated use environment.

MONITORED AND DISPLAYED ATMOSPHERIC CONSTITUENT DESIGN GOALS

Gas	Range	Detectable Limits	Accuracy
Oxygen (O_2)	60 to 200 mmHg	N/A	±5% FS
Hydrogen (H_2)	0 to 40 mmHg	10% FS	±10% FS
Carbon Dioxide (CO_2)	0 to 25 mmHg	5% FS	±5% FS

MONITORED AND DISPLAYED CONTAMINANT DESIGN GOALS

Contaminants	Range	Detectable Limits	Accuracy
Freon 11	0 to 50 ppm	5.0% FS	±10% FS
Freon 12	0 to 300 ppm	5.0% FS	±10% FS
Freon 114	0 to 300 ppm	5.0% FS	±10% FS

TEMPERATURE AND PRESSURE

The system shall perform as specified over ambient pressure from 20 to 40 inches of mercury and at ambient temperatures from 50 to 115°F.

LINE POWER

The system shall operate on 115 volt ±10%, single phase, 60 ±5% cycle alternating current (ac) power.

GENERAL SYSTEM DESIGN GUIDELINES

In general, system design shall be addressed to satisfying the operational requirements, as set forth below; however, strict adherence to these guidelines shall not be required.

a. MIL-S-901, Shock Tests, H.I. (High Impact).

b. MIL-STD-167, Mechanical Vibrations of Shipboard Equipment.

c. MIL-STD-740, Airborne and Structure Borne Noise Measurements and Acceptance Criteria of Shipboard Equipment.

d. MIL-STD-461, Electromagnetic Interference Characteristics Requirements for Equipment.

e. MIL-D-1000, Drawing, Engineering and Associated List.

Only the minimum documentation necessary for defining interface requirements, external configuration and operational characteristics shall be supplied.

DESIGN PROGRAM

Analyzer Design

The analyzer design was initiated with a study of trajectories of ions of the required mass/charge ratio with various magnet designs that were estimated to have the needed resolution without requiring a prohibitively large housing. A computer program was written to quickly calculate the most important image parameters using different magnet shapes with sharp boundaries, ignoring fringe fields. The inputs to the program consisted of object coordinates, initial velocity vector, mass/charge ratio, field strength, and magnet boundary coordinates. The program geometrically solved for the points of entry into and exit from the magnetic field, and the radius of the ion path in the field, Then the Hintenberger-Konig equations were used to compute the image location and magnification as well as the first and second order aberration coefficients. The results of this computer study with the magnet boundary finally selected is described in Project Note No. 1A, Appendix 1. In particular, the angle of the "porch" on the exit boundary was varied to study its effect on the position and aberrations of the m/e 85 and 101 beams. This porch was added to the 90° sector in order to cause the 85 and 101 beams to travel through additional magnetic field and thus bring their image points in closer to the exit boundary. This was desired in order to reduce the size of the vacuum envelope required. It was found that as the porch angle was made larger, the images did indeed move closer to the magnet boundary, however the aberrations increased.

Angles were studied from 0°, where the vacuum envelope was unacceptably large, to 28°, where the aberrations were unacceptably large. An angle of 14° was chosen as the best compromise.

Design of the analyzer proceeded after the chosen magnet was fabricated. The magnetic field was plotted in the plane of the ion trajectories using a gaussmeter on a magnet mapping fixture. The entire field from source location through the region of the collector buckets was mapped on a grid 5 mm x 5 mm. In addition, the fringe fields at the edges of the magnet were mapped with a resolution of 1 mm x 1 mm. The result of the mapping was five arrays, totaling over 2500 field measurements. With this field data, a computer program named "Monster" followed various ion trajectories through the field. For each of the seven m/e ratios, three trajectories were calculated representing the central ray, and $\pm 2°$ rays, this angle being the measured divergence of the source. When these rays are plotted, the bucket locations and α^2 aberration could be measured directly.

These computer selected bucket positions proved to be reasonably accurate. When analyzer subsystem testing was completed, it was found that the final bucket positions were within 0.050" in all cases except for 85 and 101. For some reason these two buckets required 0.250" movement outward along the trajectory to find the best focus. By contrast, the bucket positions computed assuming a perfect field with no fringing, by means of the Hintenberger-Konig relations, were over 1/2 inch off in every case.

The results of these computations are listed in Project Note No. 3, including collector slit widths for zero crosstalk at the specified resolutions. Several trajectories are plotted out in Figure 1. Details of the computations for m/e 85 and 101 are in Project Note No. 1. In these cases we are actually looking at beams that are three mass units wide, in order to include 85 - 87 in the same collector, and 101 - 103 in the same collector. This somewhat complicates the situation.

Included in the analyzer design was a study of the effect of the ion source magnetic shield on the location of the m/e 2 collector. In the past it has been suspected that the subsequent addition of this, or other magnetic shields changed the fringe field sufficiently to move the m/e 2 image a large amount. As shown in the note, in this design the problem is not significant.

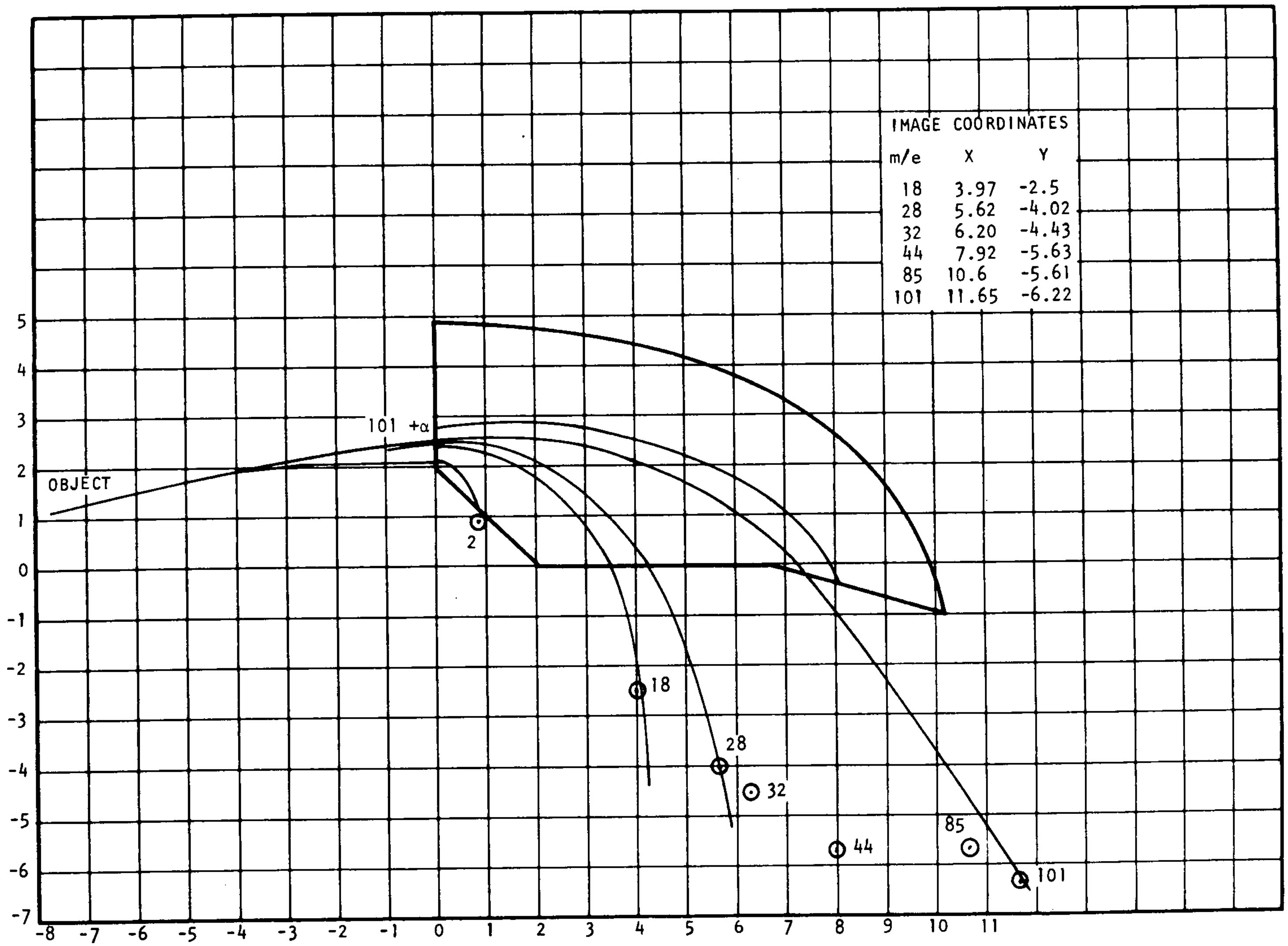

FIGURE 1. Results of Computer Ray Tracing Through the Magnetic Field Which Was Measured on the Magnet Fabricated From the Design of Project Note No. 1, Appendix II

Since the ion source from contract NAS9-9799 was used directly, very little design effort was required to adapt it to this analyzer. The Z-axis focus lens was changed to adapt it to this new geometry and other minor modifications were made to mount it in the housing and adapt it to the varian leak. The initial voltages used for the power supply design were taken from the range of experience in NAS9-9799. The various parameters related to the source are computed in Project Notes 2, 6 and 7. The same computations, as they relate to the freons, are covered in Project Notes 1 and 5. The automatic subtraction circuits which correct the various freon combinations follow very closely the factors calculated in Note 5. The details of the operation of the freon logic sequencing circuits are further discussed in the Operations and Maintenance Manual, on pages I-29 through I-32.

The sample inlet system was of conventional design quite similar to previous systems and so very little design effort was required other than the physical layout. A few calculations of pressure drops in the filters, and delays through long transport lines are included in Project Note No. 11. The transport pump, manufactured by Metal Bellows Corporation, was chosen after an extensive market survey. It was chosen for its reliability and ruggedness, and has the added feature of quiet operation when compared to alternate pumps.

TEST PROGRAM

Component Tests

The analyzer subsystem component tests were principally concerned with testing the inlet leak valve to measure its temperature coefficient. It is the steep temperature coefficient of the valve that acts as the automatic shut-off when power is lost. In addition, this property of the valve makes temperature control an absolute necessity. The leak rate vs setting of the Varian leak valve is shown in Figure 2. It can be seen that there is a sharp break in the curve at a leak rate of about 10^{-8} torr-liters/sec. The operating point for the leak on our instrument is 5×10^{-6} torr-liter/sec. Therefore a slight change in the knob setting, or as we have found, a slight decrease in temperature is sufficient to decrease the conductance of the leak by over two orders of magnitude. The leak valve test results are presented in Project Note No. 9. It is shown there that of the four valves tested, two closed completely when the heater lost power, and two closed sufficiently that many hours of power off could be tolerated before the pressure rose far enough to require rough pumping the analyzer. Also shown in Note 9 is the thermal coefficient as a function of temperature. The same break as found in the setting curve is found in the temperature coefficient curve and is undoubtedly due to the same mechanical characteristics.

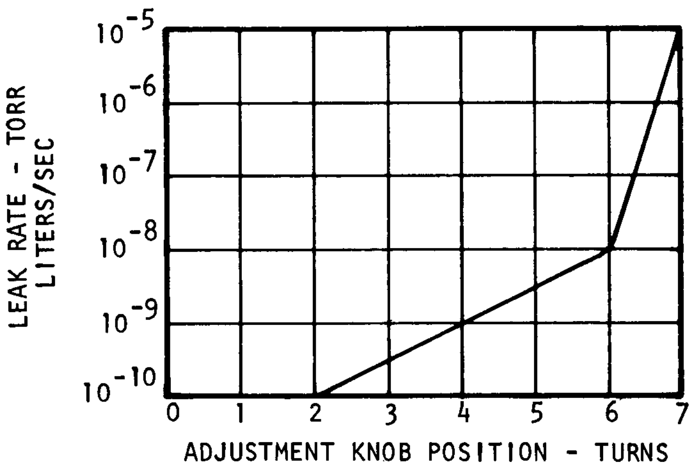

THE RATE-OF-CHANGE OF LEAK RATE IN RELATION TO ROTATION OF THE ADJUSTMENT KNOB CHANGES AT APPROXIMATELY 10^{-8} TORR-LITERS/SEC AS SHOWN ON THE GRAPH. THIS RESULTS IN VERY FINE CONTROL AT LOW LEAK RATES, AND A MORE RAPID RESPONSE TO CHANGE AT LEAKS OVER 10^{-8} TORR-LITERS/SEC.

FIGURE 2. Control and Response

Analyzer Subsystem Tests

The analyzer subsystem, consisting of ion pump, analyzer, ion source and leak is subjected to a series of tests designed to examine each of the functions of the analyzer as independently as possible. While performing these tests the voltages and mechanical adjustments are optimized. A list of the principal steps is given below:

(1) The analyzer is carefully inspected during assembly.

(2) The assembled analyzer tube is leak checked, checked for shorts, and pumped down on a laboratory support vacuum system.

(3) The ion source filaments are turned on in a standard operating mode for outgassing and warmup to assure maximum life. Operating characteristics are recorded, including current and voltage.

(4) The instrument is subjected to a bakeout to obtain maximum cleanliness and to minimize any possibility of contamination.

(5) Each electron gun is tested with a variety of voltages and emission current levels to find the maximum transmission efficiency for electrons to the anode of the ion source.

(6) The analyzer magnet is put in place and its effect upon the electron gun operation is checked.

(7) A mass scan is then obtained on a convenient collector and the ion current is then monitored to tune up the ion source.

(8) The ion focusing electrodes are tuned for maximum ion source output.

(9) The side electrodes in the ionizing region are tuned for maximum ion current output. This corresponds to centering the electron beam in the ionizing region.

(10) The ion source sensitivity $\Delta I^+/\Delta p$ is measured using a nitrogen sample, and monitoring the I^+_{28} output.

(11) The Z-axis focus electrodes are tuned. This should be done on m/e 18, m/e 28 and m/e 44.

(12) The analyzer is tuned for maximum resolution at each mass position by adjusting the magnet position in two directions of translation. Successive mass scans are made to determine the resolution and peak shape.

(13) The alignment of the collectors is checked to see that the masses of interest fall into their respective collectors at the same ion energy. Tolerance to ion energy variation is also measured.

(14) The collector flange is removed and the position of the collectors are adjusted so that best focus and collection of ions at the same energy is achieved. Several iterations may be required.

(15) The voltage is scanned with the F114 stepping switch and the m/e 135 peak is scanned on the 101 collector.

(16) The analyzer differential pumping ratio is checked by introducing N_2 at the roughing valve through a leak, and measuring N_2^+ vs I_p^+.

(17) Linearity of N_2^+ vs I_{AN} from 0 to 40 μA and vs inlet pressure from 0 - 1000 torr is measured.

(18) Background currents were measured at all collectors.

Two of the peak alignment scans are shown in Figures 3 and 4. Figure 3 shows an early scan before best magnet location had been chosen and before collector movements. Figure 4 shows the final peaks scan.

Once the analyzer subsystem is complete, and each electronic subsystem is completely tested, the system is integrated for system test. The system test consists of testing all those parameters which specify the overall system performance. Throughout the electronics subsystems there are numerous potentiometer adjustments and "select-at-test" resistor values which are adjusted during the system test phase. In addition, all tests and adjustments were repeated a second time with each instrument for the spare electronics circuit boards.

Sea Trial

Before the final acceptance testing of the instrument, one system was subjected to a trial on board the Submarine USS Pintado during two short voyages. The results of these sea trials are shown in Figures 5 and 6. The bottom trace of each of these figures shows that the sum of the partial pressures of the measured constituents stayed within 1 percent of the total pressure at all times. The CO results included here are measured by an MSA device, not associated with the Perkin-Elmer Atmospheric Contaminant Sensor.

Acceptance Test

After S/N 01 was returned from the sea trial, the two units were subjected to the final acceptance test. This test, with results is included here as Appendix 2.

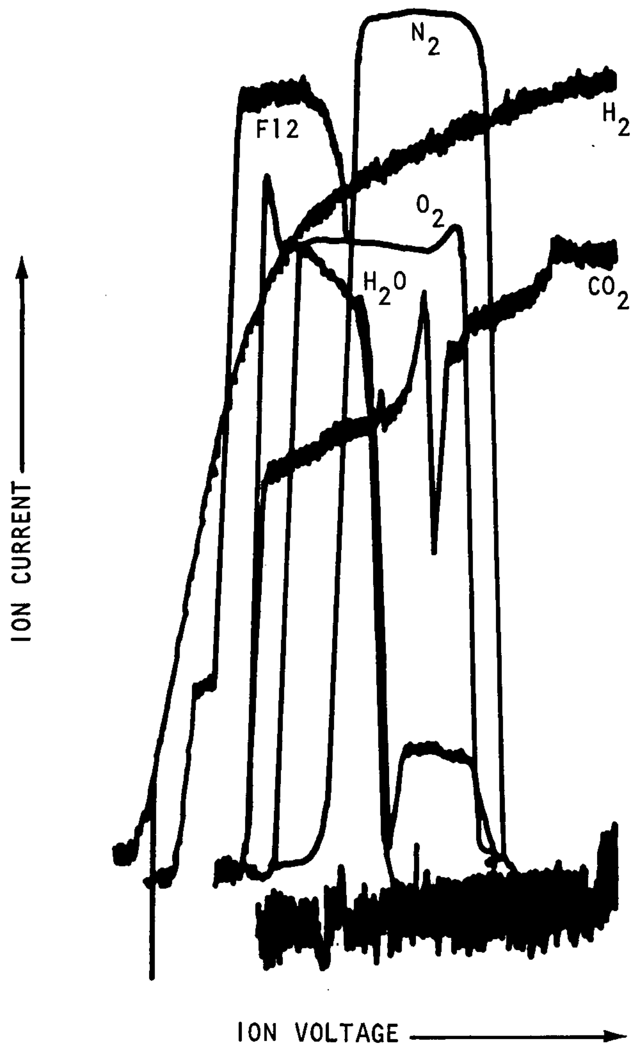

THE VOLTAGE AXIS IS THE SAME FOR ALL TRACES. TEST GASES AND GAIN OF THE CURRENT AXIS IS VARIED BETWEEN TRACES IN ORDER TO BEST EVALUATE PEAK SHAPE AND LOCATION. THESE ARE PRELIMINARY TRACES BEFORE MAGNET AND COLLECTOR ADJUSTMENTS.

FIGURE 3. Collector Currents vs Ion Accelerating Voltage

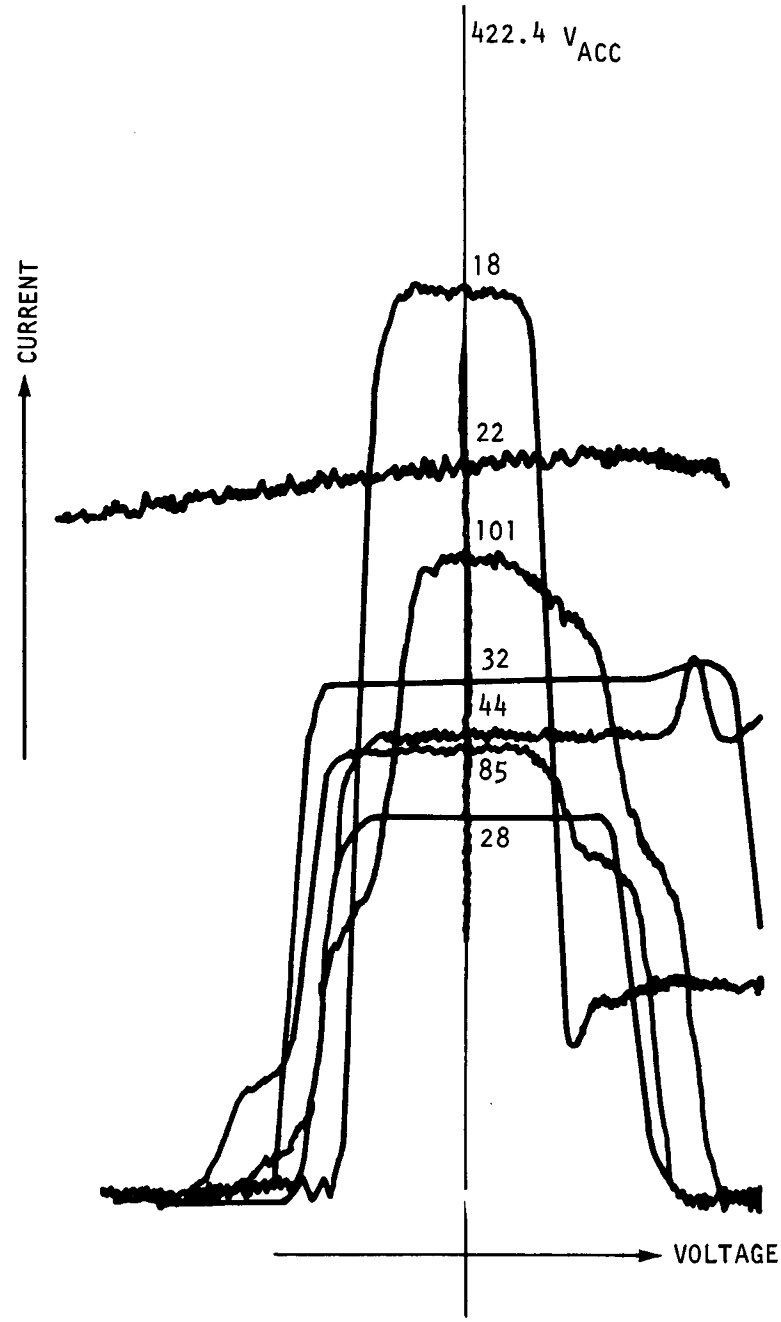

SIMILAR TO FIGURE 3 EXCEPT THAT THESE ARE THE FINAL TRACES AFTER BEST MAGNET POSITION AND COLLECTOR POSITIONS ARE INCORPORATED.

FIGURE 4. Collector Currents vs Ion Accelerating Voltage

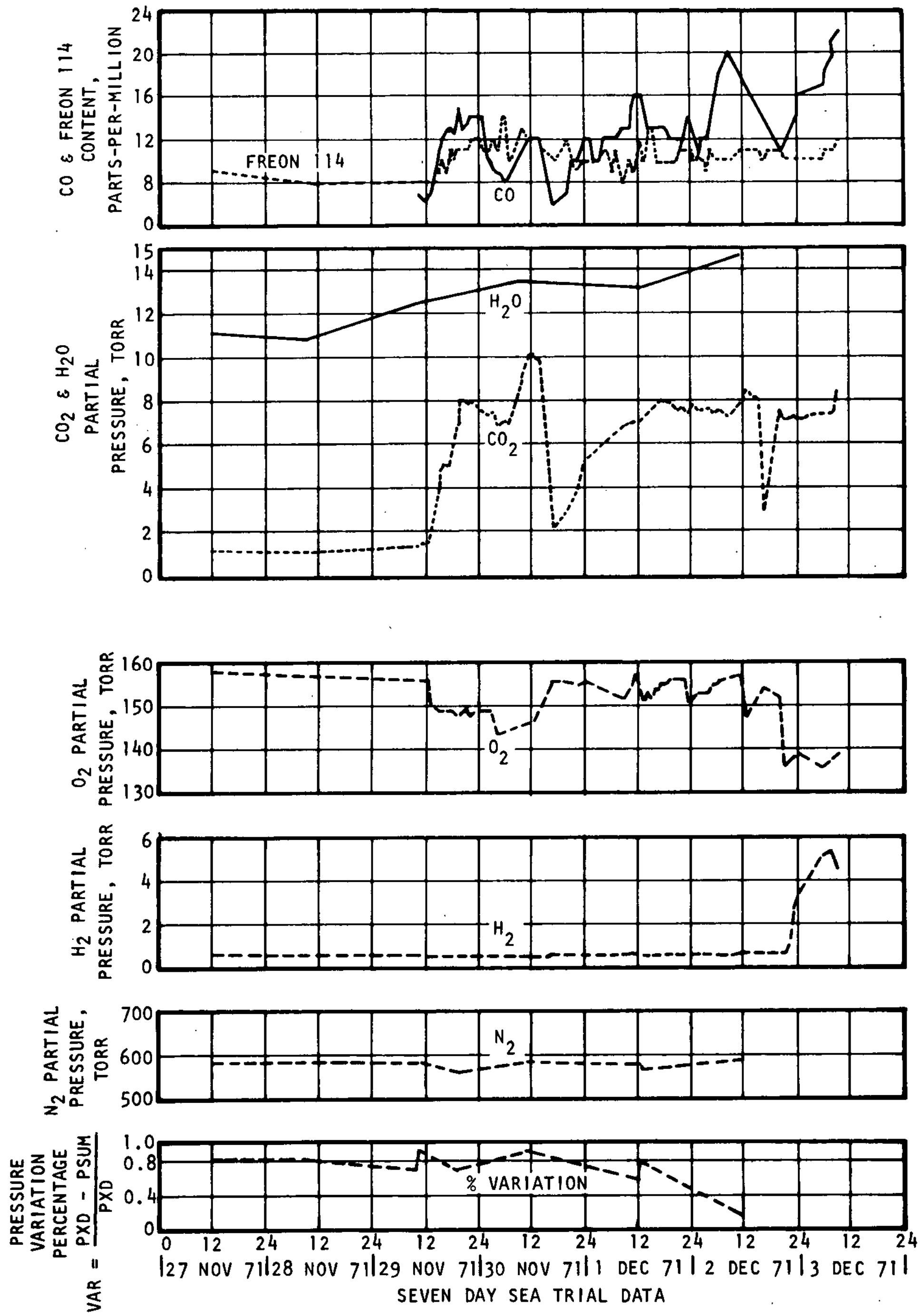

FIGURE 5. Seven Day Sea Trial Data

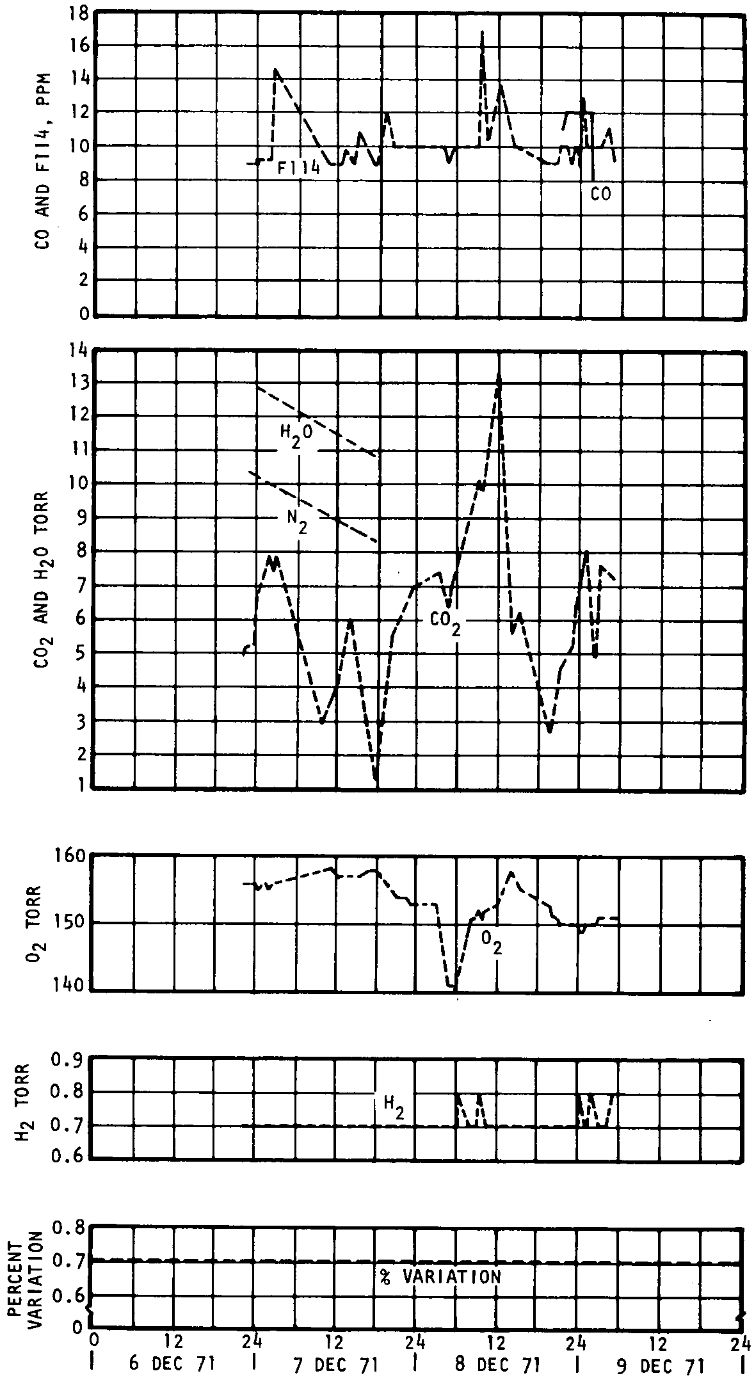

FIGURE 6. Seven Day Sea Trial Data